Molecular and cellular characterization of cardiac overload-induced hypertrophy and failure

Umar, S.

Chapter 4

Activation of signaling molecules and matrix metalloproteinases in right ventricular myocardium of rats with pulmonary hypertension

S. Umar
M. H. M. Hessel
P. Steendijk
W. H. Bax
C. I. Schutte
M. J. Schalij
E. E. Van der Wall
D.E. Atsma
A. van der Laarse

Pathology – Research and Practice 2007;203:863-872

Abstract

Background: Pulmonary hypertension induces right ventricular (RV) overload that is transmitted to cardiomyocytes via integrins that activate intracellular messengers, including focal adhesion kinase (FAK) and neuronal nitric oxide synthase (NOS1). We investigated whether RV hypertrophy (RVH) and RV failure (RVF) were associated with activation of FAK, NOS1 and matrix metalloproteinases (MMPs).

Methods: Rats were treated without (RVC) or with monocrotaline in low dose (30 mg/kg) to induce RVH and in high dose (80 mg/kg) to induce RVF. After ≈30 days, RV function was determined using combined pressure-conductance catheter. After sacrifice, FAK, NOS1, their phosphorylated forms (FAK-P and NOS1-P), MMP-2 and MMP-9 were quantified in RV myocardium by immunohistochemistry.

Results: In RVH and RVF, RV weight/ body weight increased by 36% and 109%, whereas RV ejection fraction decreased by 23% and 57% vs. RVC, respectively. FAK-P and FAK-P/FAK were highest in RVH (2.87±0.12 and 2.52±0.23 fold compared to RVC, respectively) and slightly elevated in RVF (1.76±0.17 and 1.15±0.13 fold compared to RVC, resp.). NOS1-P and NOS1-P/NOS1 were increased in RVH (1.63±0.12 and 3.06±0.80 fold compared to RVC, resp.) and RVF (2.16±0.03 and 3.30±0.38 fold compared to RVC, resp.). MMP-2 was highest in RVH and intermediate in RVF (3.50±0.12 and 1.84±0.22 fold compared to RVC, resp.). MMP-9 was elevated in RVH and RVF (2.39±0.35 and 2.92±0.68 fold compared to RVC, resp.).

Conclusions: Activation of FAK in RVH points to an integrin-dependent hypertrophic response of the myocardium. Activation of NOS1 in failing RV suggests a role of excessive NO in development of failure and activation of MMPs leading to ventricular remodeling.

Key words:
Hypertrophy; heart failure; focal adhesion kinase; neuronal nitric oxide synthase; matrix metalloproteinase

Abbreviations: FAK, focal adhesion kinase; nNOS, neuronal nitric oxide synthase; NOS1, neuronal nitric oxide synthase; NO; nitric oxide; MMP, matrix metalloproteinase; ECM, extracellular matrix; SR, sarcoplasmic reticulum; RyR, ryanodine receptor; MCT, monocrotaline; ROS, reactive oxygen species; CHF, congestive heart failure; RV, right ventricle; LV, left ventricle; IVS, interventricular septum; RVC, right ventricular control; RVH, right ventricular hypertrophy; RVF, right ventricular failure; PBS, phosphate-buffered saline; LVH, left ventricular hypertrophy; LVEF, left ventricular ejection fraction; LVESV, left ventricular end systolic volume; SNP, Sodium nitroprusside.

Introduction

Pulmonary hypertension is a condition that causes overloading of the right ventricle (RV). The forces of overload are transferred to the cardiomyocytes via integrins, a family of transmembrane adhesion receptors. Integrin signaling occurs via a large array of intracellular messenger systems, including focal adhesion kinase (FAK) [25, 26]. FAK is a cytoplasmic tyrosine kinase that discretely localizes to membrane regions that attach to the extracellular matrix (ECM), called focal adhesions. FAK transmits signals from the ECM via integrins to the cytoskeleton and particular cytoplasmic proteins. Stimulation of integrins and FAK leads to a hypertrophic response in cardiomyocytes [17].

Earlier we have shown that integrin stimulation was associated with immediate FAK phosphorylation and delayed phosphorylation of neuronal nitric oxide synthase (nNOS, NOS1) [32, 33]. NOS1 is located on the sarcoplasmic reticulum (SR) of cardiomyocytes, and is considered to modify SR function via nitrosylation of the ryanodine receptor (RyR) which is the calcium release site of the SR [3, 19, 29, 34, 38]. NO and reactive oxygen species (ROS) produce peroxynitrite, known to activate matrix metalloproteinases (MMPs) [20, 35] that are involved in ventricular remodeling [27]. The exact role of the NO formed in the failing myocardium is not yet fully elucidated. We hypothesize that signaling pathways involved in myocardial hypertrophy and failure are NO-dependent, including NO-dependent MMP activation leading to ventricular remodeling.

A frequently used model to study functional, structural and molecular changes associated with compensated RV hypertrophy (RVH) and RV failure (RVF) is the rat treated with monocrotaline (MCT), a pyrrolizidine alkaloid [13, 16]. MCT selectively injures the vascular endothelium of the lung and induces pulmonary vasculitis [37]. Muscularization and hypertrophy of media of pulmonary arteries lead to increased vascular resistance and increased pulmonary arterial pressure [8, 22]. MCT-induced pulmonary hypertension is associated with the development of compensated RVH progressing to RVF within weeks, depending on the dose of MCT and the age of the rats [7, 15, 36]. Previous studies have shown selective induction of either RVH or RVF after 4 weeks of treatment with a low dose (30 mg/kg body weight) or a high dose (80 mg/kg body weight) of MCT, respectively [7, 14].

In the rat model of MCT-induced pulmonary hypertension, we determined activation of FAK, NOS1, immunoreactive MMP-2 and MMP-9 in RV myocardium to compare differences with respect to their activation patterns between controls, RVH and RVF. To test whether NO stimulates expression of MMP-2 and MMP-9, neonatal rat ventricular cardiomyocyte cultures were treated without and with the NO-donor sodium-nitroprusside for 24 h, followed by quantitative determination of immunoreactive MMP-2 and MMP-9.

Materials and Methods

Animal model

All animals were treated in accordance with the national guidelines and with the approval of the Animals Experiments Committee of the Leiden University Medical Center. A total of 14 male Wistar rats (Harlan, Zeist, the Netherlands) weighing 200-250 g were randomly assigned to three groups. Animals received a single subcutaneous injection of MCT (Sigma-Aldrich, Zwijndrecht, the Netherlands) diluted in phosphate-buffered saline (PBS) in a low dose (30 mg/kg body weight, n=5; RVH group) or in a high dose (80 mg/kg body weight, n=5, RVF group). Control rats (RVC, n=4) were injected with an equal volume of PBS.

Hemodynamics

After 4 weeks of MCT administration RV pressure and volume signals were recorded by combined pressure-conductance catheter. To that purpose rats were sedated by inhalation of a mixture of isoflurane (4%) and oxygen. General anesthesia was administered by intraperitoneal (i.p.) injection of a fentanyl-fluanison-midazolam mixture in a dose of 0.25 mL/100 g body weight. The mixture consisted of 2 parts Hypnorm® (0.315 mg/mL fentanyl + 10 mg/mL fluanison, VitalPharma, Maarheeze, the Netherlands), 1 part Dormicum® (5 mg/mL midazolam, Roche, Mijdrecht, the Netherlands) and 1 part saline. After tracheotomy the animals were ventilated mechanically using a pressure-controlled respirator and a mixture of air and oxygen.

After midsternal thoracotomy a combined pressure-conductance catheter (SPR-878, Millar Instruments, Houston, TX, USA) was introduced via the apex into the RV and positioned along the long axis of the RV. The catheter was connected to a Sigma-SA signal processor (CD Leycom, Zoetermeer, the Netherlands) and RV pressures and volumes were recorded digitally. All data were acquired using Conduct-NT software (CD Leycom) at a sample rate of 2000 Hz and analysed off-line by custom-made software. The volume signal was calibrated using an ultrasonic flow probe (Transonic Systems, Maastricht, the Netherlands) around the ascending aorta, essentially as described by Hessel et al. [14]..

Heart rate, RV stroke volume, cardiac output, RV end-diastolic volume, RV end-systolic volume, RV ejection fraction, RV end-diastolic pressure, RV peak systolic pressure and RV end-systolic pressure were determined from pressure-volume loops.

Tissue preparation

Immediately after hemodynamic measurements, hearts were rapidly dissected and weighed. The RV, left ventricle (LV) and interventricular septum (IVS) were cut free, weighed, fixed in 4% formaline for more than 24 h, and embedded in paraffin. Subsequently, 4 µm thick sections of the RV tissue were cut and deparafinized in Ultraclear® (Klinipath, Duiven, the Netherlands) for 5 min. Sections were rehydrated in decreasing graded alcohols (100-25%) followed by two 5-min washes in distilled water and TBS (10 mmol/L Tris-HCl, 150 mmol/L NaCl, pH 8.0).

Immunohistochemistry

Sections cut from RV myocardium of RVC, RVH and RVF groups were stained for FAK, FAK-P, NOS1, NOS1-P, MMP-2 and MMP-9. Rabbit anti-FAK and anti-FAK-P antibodies were from Santa Cruz Biotechnology (Santa Cruz, CA, USA). Rabbit anti-NOS1 and anti-NOS1-P antibodies were from Upstate (Charlottesville, VA, USA). Mouse anti-MMP-2 antibody and mouse anti-MMP-9 antibody were from Chemicon International (Temecula, CA, USA).

Secondary antibodies used were donkey anti-rabbit IgG conjugated to Texas Red (Santa Cruz), goat anti-rabbit IgG conjugated to FITC (Sigma-Aldrich), goat anti-mouse IgG conjugated to FITC (Sigma-Aldrich), and donkey anti-mouse IgG conjugated to Cy3 (Jackson Immuno Research Labs, West Grove, PA, USA).

Sections were incubated in a solution of 0.1% sodium citrate and 0.5% Triton X-100 at room temperature for 3 min. After washing with distilled water and TBS solution, sections were incubated for 20 min in 10% serum derived from the same animal species in which the secondary antibody was raised, in TBSB (TBS containing 0.05 mg/mL baseral). After removal of blocking serum, the sections were incubated overnight at 4^{o}C with the primary antibody diluted in TBSB. After removal of the primary antibody and washing three times with TBS, sections were incubated with secondary antibody diluted in TBSB for 1 h at room temperature in the dark. Subsequently, sections were washed three times with TBS, and counterstained with 0.01 mg/mL Hoechst 33342 (Molecular Probes, Eugene, OR, USA) for 10 min at room temperature in the dark. Sections were washed three times with TBS and mounted on microscope glass using Vectashield (Vector Laboratories, Burlingame, CA, USA). Sections were photographed in a fluorescence microscope (Nikon Eclipse, Nikon Europe, Badhoevedorp, the Netherlands) equipped with a 100x oil-immersion objective and a digital camera (Nikon DXM 1800). Images were analyzed using Image-Pro Plus software (Media Cybernetics, Silver Spring, MD, USA) that allows quantification of blue, green and red separately. Per section 5 images were acquired and analyzed to compensate for variations within a section.

Preparation of neonatal rat ventricular cardiomyocytes and immunocytochemistry of cellular MMP2 and MMP9

Neonatal (2-day-old) rat ventricular cardiomyocytes were prepared as described before [24]. Cells were plated in 6-well plates containing per well a collagen-coated glass cover-slip and were grown in growth medium consisting of DMEM and Ham's F10 (1:1, $^{v}/_{v}$), 2.5% horse serum, 100 U/mL penicillin and 100 µg/mL streptomycin (all from Invitrogen, Breda, the Netherlands). Three days after isolation, the cardiomyocytes were used for experiments. At termination of the experiment, the cover-slips were prepared for immunofluorescence microscopy according to a protocol described before [33]. Briefly the cover-slip was washed, incubated with PBS containing 1% formalin for 30 min, washed, incubated with PBS containing 0.1% Triton X-100 for 10 min, washed, and incubated overnight with first antibody (200x diluted in PBS + 1% FBS) at 4^{o}C. Primary antibodies raised against MMP2 and MMP9 were the same as used with the myocardial tissue sections. After washing, the cells were incubated with secondary rabbit anti-mouse Alexa568-conjugated antibody (Molecular Probes; 400x diluted in

PBS + 1% FBS) for 1 h. After washing, the cultures were incubated with 10 µg/mL Hoechst 33342 for 10 min. After washing, cells were mounted on microscope slides using Vectashield. Microscope and camera were the same as used with the myocardial tissue sections.

Statistics

Data are expressed as mean ± SD. The effect of treatment (RVC, RVH and RVF) was evaluated by one-way analysis of variance (ANOVA) followed by Bonferroni's *post hoc* test. Correlations were determined using a parametric test (Pearson). Differences were considered significant at $p<0.05$. SPSS12 for Windows (SPSS Inc, Chicago, IL, USA) was used for statistical analysis.

Results

Body and heart weights

Table 1 summarizes characteristics of the animals at the day they were sacrificed. Immediately after hemodynamic measurements, hearts were rapidly dissected and weighed. Body weight of RVF rats was significantly lower than that of RVC and RVH rats ($p<0.05$ vs. RVC and RVH). RV weight of RVF animals was significantly higher than that of RVC and RVH rats ($p<0.05$ vs. RVC and RVH). The degree of RV hypertrophy was determined as the ratio of RV weight over the body weight. This hypertrophy parameter was increased (by +36%) in RVH ($p<0.05$ vs. RVC) and was significantly higher in RVF (+109% compared to RVC, +53% compared to RVH, both $p<0.05$). Furthermore, weight of RV as a fraction of total ventricular weight was significantly increased in RVH (+27% compared to RVC) and in RVF (+54% compared to RVC, +21% compared to RVH, both $p<0.05$) confirming RV hypertrophy in both MCT-treated groups. Conversely, there was no significant increase in the ratios of (LV+IVS) weight over body weight and (LV+IVS) weight over total ventricular weight in RVH and RVF compared with RVC (Table 1).

Table 1. General and cardiac characteristics of RVC, RVH and RVF animals

	RVC (n=4)	**RVH** (n=5)	**RVF** (n=5)
Body weight (g)	370 ± 24.71	365.2 ± 26.52	319.8 ± 24.04*#
RV weight (g)	0.24 ± 0.03	0.33 ± 0.03*	0.44 ± 0.08*#
(LV+IVS) weight (g)	0.85±0.1	0.84±0.08	0.85±0.06
VW (RV+LV+IVS) (g)	1.09 ± 0.12	1.17 ± 0.11	1.29 ± 0.12*
RV/BW ($mg.g^{-1}$)	0.66±0.08	0.90±0.05*	1.38±0.3*
RV/VW	0.22±0.02	0.28±0.01*	0.34±0.03*#
VW/BW ($mg.g^{-1}$)	2.94 ± 0.13	3.2 ± 0.16*	4.05 ± 0.47*#
(LV+IVS)/BW ($mg.g^{-1}$)	2.28± 0.12	2.3± 0.13	2.67± 0.19
(LV+IVS)/VW	0.77±0.02	0.72±0.01	0.66±0.04

* $p<0.05$ vs. RVC
# $p<0.05$ vs. RVH
abbreviations: RVC, RV control; RVH, RV hypertrophy; RVF, RV failure; RV, right ventricle; VW, Ventricular weight; BW, body weight; LV, left ventricle; IVS, interventricular septum

Right ventricular function

Results of combined pressure-conductance catheter measurements are summarized in Table 2.

RV ejection fraction (RVEF) was 53.2±5.7 % in RVC, 40.9±9.6 % in RVH and 22.7±6.9 % in RVF (p<0.05 vs. RVC) while RV end-diastolic pressure was 1.4±0.4 mmHg in RVC, 3.6±0.4 mmHg in RVH and 8.0±1.5 mmHg in RVF (p<0.05 vs. RVC and RVH) confirming RV failure in the RVF group. Furthermore, in RVH rats, cardiac output (CO) and stroke volume (SV) were maintained, indicating a compensatory state at the expense of increased RV end-diastolic and end-systolic volumes and increased RV filling pressure (all p<0.05 vs. RVC).

Table 2. Cardiac and right ventricular function of RVC, RVH and RVF animals

	RVC (n=4)	**RVH** (n=5)	**RVF** (n=5)
Heart rate (min^{-1})	407 ± 24	397 ± 22	259 ± 77
Stroke volume (µL)	145 ± 11.4	162 ± 13.1	177 ± 26.5
Cardiac output ($mL.min^{-1}$)	58.3 ± 1.2	64.0 ± 5.3	41.8 ± 7.3
RV end-systolic volume (µL)	134 ± 29.2	265 ± 52.1	690 ± 186*
RV end-diastolic volume (µL)	276 ± 40.7	409 ± 47.2	833 ± 197*
RV ejection fraction (%)	53.2 ± 5.7	40.9 ± 9.6	22.7 ± 6.9*
RV end-systolic pressure (mmHg)	25.9 ± 4.1	28.6 ± 3.7	46.7 ± 10.9
RV end-diastolic pressure (mmHg)	1.4 ± 0.4	3.6 ± 0.4	8.0 ± 1.5*#

* p<0.05 vs. RVC
# p<0.05 vs. RVH
abbreviations: RVC, RV control; RVH, RV hypertrophy; RVF, RV failure; RV, right ventricle

FAK phosphorylation

FAK is involved in the hypertrophic response of cardiomyocytes and undergoes autophosphorylation on integrin stimulation. To assess the activation of FAK in our RV hypertrophy and failure model, we quantified its phosphorylation and FAK-P/FAK ratio by immunohistochemical techniques (Fig. 1). Myocardial FAK-P concentration was highest in RVH (2.87±0.12 fold higher than the corresponding value in RVC, p<0.05 vs. RVC) and less elevated in RVF (1.76±0.17 fold higher than the corresponding value in RVC, p<0.05 vs. RVC) (Fig. 1b). The ratio of FAK-P/FAK was also found to be the highest in RVH (2.52±0.23 fold higher than the corresponding value in RVC, p<0.05 vs. RVC) and hardly elevated in RVF group (1.15±0.13 fold higher than the corresponding value in RVC) (Fig. 1c). Hence there was an increase in phosphorylation of FAK as well as FAK-P/FAK ratio in RV hypertrophy group.

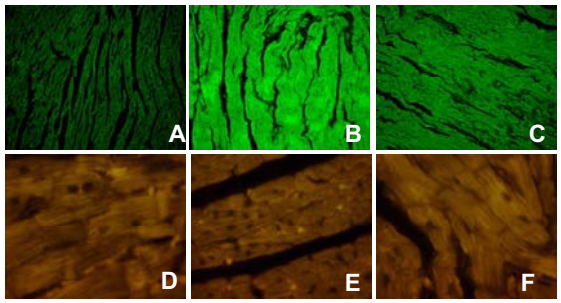

Figure 1a. Immunofluorescence images of phosphorylated FAK in RVC (A), RVH (B) and RVF (C) using an FITC labeled secondary antibody. All images were taken at 20x magnification. **.** Immunofluorescence images of total FAK in RVC (D), RVH (E) and RVF (F) are also shown. Images were taken at 100x magnification.

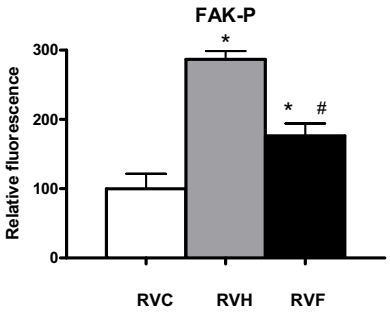

Figure 1b. Relative fluorescence of FAK-P in RVC, RVH and RVF.
(* *p*< 0.05 vs. RVC; # *p*<0.05 vs. RVH)

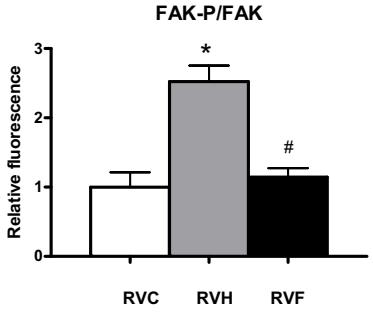

Figure 1c. Ratios of the relative fluorescence of phosphorylated FAK/ total FAK (FAK-P/FAK) in RVC, RVH and RVF.
(* p< 0.05 vs. RVC; # p<0.05 vs. RVH)

NOS1 phosphorylation

NOS1 is another signaling protein thought to be involved in integrin stimulation. We assessed NOS1 phosphorylation by quantification of immunofluorescence (Fig. 2a). Myocardial NOS1-P concentration was found to be increased in RVH (1.63±0.21 fold higher than the the corresponding value in RVC, $p<0.05$ vs. RVC) and RVF (2.16±0.03 fold higher than the corresponding value in RVC, $p<0.05$ vs. RVC and RVH) (Fig. 2b).The ratio of NOS1-P/NOS1 was markedly elevated in RVH (3.06±0.80 fold higher than the corresponding value in RVC, $p<0.05$ vs. RVC) and RVF (3.30±0.38 fold higher than the corresponding value in RVC, $p<0.05$ vs. RVC) (Fig. 2c), showing elevated NOS1 phosphorylation state with RV hypertrophy and failure.

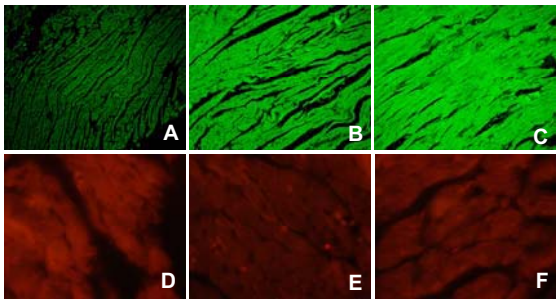

Figure 2a. Immunofluorescence images of phosphorylated NOS1 in RVC (A), RVH (B) and RVF (C) using an FITC labeled secondary antibody. All images were taken at 20x magnification. Immunofluorescence images of total NOS1 in RVC (D), RVH (E) and RVF (F) are also shown. Images were taken at 100x magnification.

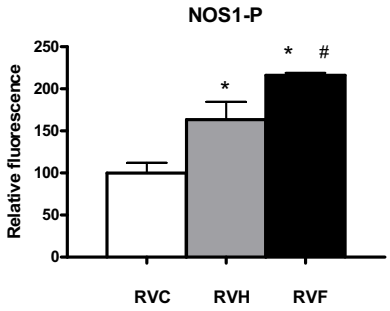

Figure 2b. Relative fluorescence of NOS1-P in RVC, RVH and RVF.
(* p< 0.05 vs. RVC; # p<0.05 vs. RVH)

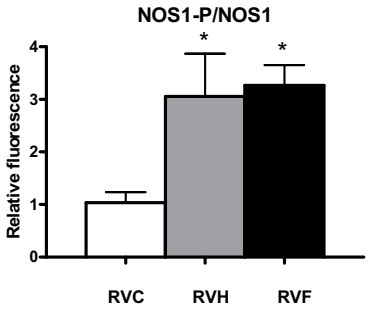

Figure 2c. Ratios of the relative fluorescence of phosphorylated NOS1/ total NOS1 (NOS1-P/NOS1) in RVC, RVH and RVF.
(* p< 0.05 vs. RVC)

Activation of MMP-2 and MMP-9 by exogenous NO

Neonatal rat ventricular cardiomyocytes were incubated with 10 µg/mL sodium-nitroprusside (SNP) for 24 h and subsequently analysed for cellular MMP2 and MMP9 immunoreactivity by immunofluorescence microscopy. This dose of NO-donor caused an increase of MMP2 by 222% ($p<0.001$) and an increase of MMP9 by 72% ($p<0.001$) in 24 h (Figure 3), indicating that NO stimulates MMP2 and MMP9 expression.

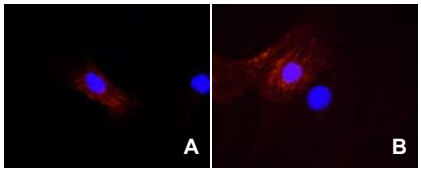

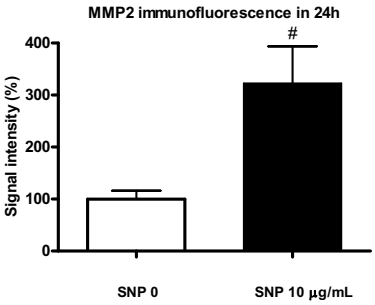

Figure 3a. Immunofluorescence images of MMP2 in rat ventricular cardiomyocytes incubated without (SNP 0, A) and with 10 µg/mL sodium-nitroprusside (SNP 10, B) for 24 h. Quantitative analysis of signal intensities is presented.
(# p<0.001 vs. SNP0)

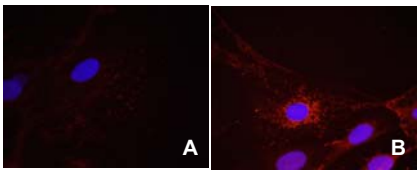

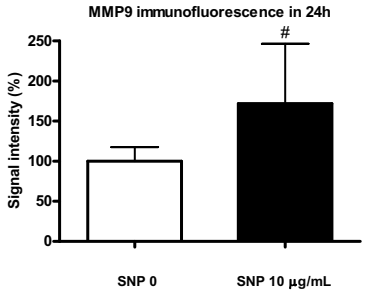

Figure 3b. Immunofluorescence images of MMP9 in rat ventricular cardiomyocytes incubated without (SNP 0, A) and with 10 µg/mL sodium-nitroprusside (SNP 10, B) for 24 h. Quantitative analysis of signal intensities is presented.
(# p<0.001 vs. SNP0)

Activation of MMP-2 and MMP-9 in hypertrophied and failing RV

MMP-2 and MMP-9 are the most commonly implied MMPs in ventricular failure and remodeling. We assessed the activation of RV myocardial immunoreactive MMP-2 and MMP-9 in our rat model of heart failure by immunohistochemical methods. We found that myocardial MMP-2 concentration (Fig. 4b) was the highest in RVH (3.50±0.12 fold higher than the corresponding value in RVC, $p<0.05$ vs. RVC) and intermediate in RVF (1.84±0.22 fold higher than the corresponding value in RVC, $p<0.05$ vs. RVC).

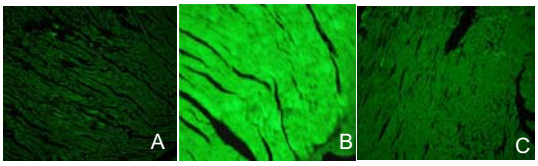

Figure 4a. Immunofluorescence images of immunoreactive MMP-2 in RVC (A), RVH (B) and RVF (C) using an FITC labeled secondary antibody. All images were taken at 20x magnification.

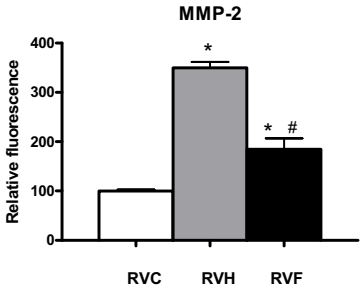

Figure 4b. Relative fluorescence of MMP-2 in RVC, RVH and RVF.
(* p< 0.05 vs. RVC; # p<0.05 vs. RVH)

Myocardial MMP-9 concentration was significantly increased both in RVH and RVF (2.39±0.35 and 2.92±0.68 fold higher than the corresponding values in RVC, respectively, both p<0.05 vs. RVC) (Fig 5b). Hence we found an activation of both MMP-2 and MMP-9 in the remodeling RV myocardium.

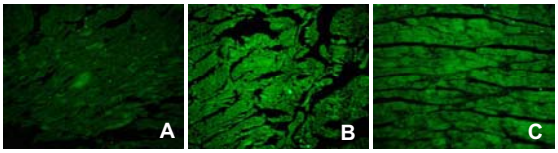

Figure 5a. Immunofluorescence images of immunoreactive MMP-9 in RVC (A), RVH (B) and RVF (C) using an FITC labeled secondary antibody. All images were taken at 20x magnification.

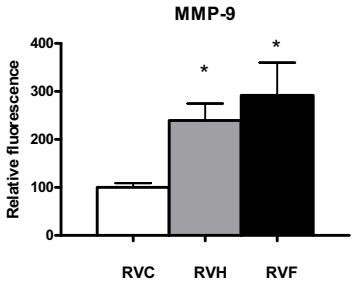

Figure 5b. Relative fluorescence of MMP-9 in RVC, RVH and RVF. (* $p < 0.05$ vs. RVC)

Discussion

In the present study we showed that in a rat model of pulmonary hypertension, there is an activation of signaling proteins FAK and NOS1 with concurrent activation of matrix metalloproteinases MMP-2 and MMP-9 in the RV myocardium. In rat cardiomyocyte cultures, exogenous NO was found to activate cellular MMP-2 and MMP-9. In the rat model of pulmonary hypertension, we found a dose-dependent effect of the toxin, monocrotaline, on the pulmonary vasculature, leading to compensated RV hypertrophy in RVH group and RV failure in RVF group.

For the RV, pulmonary hypertension means increased afterload. The forces associated with increased afterload are transferred to the cardiomyocytes of the RV myocardium via integrins, a family of transmembrane adhesion receptors. Integrins couple the proteins of the extracellular matrix to the cellular cytoskeleton and other specific proteins, like FAK. Stimulation of integrins elicits cellular signaling pathways via a large array of cellular messenger systems, including autophosphorylation of FAK. Stimulation of integrins and FAK leads to a hypertrophic response in cardiomyocytes [17]. Integrin-mediated signaling activates protein tyrosine kinases such as FAK and Src, and results in the activation of the ERK2 and JNK1 pathways which in turn activate transcription factors relevant to MMP transcriptional regulation [23, 18].

Bayer *et al.* [4] have shown that FAK levels increased during established phase of compensatory left ventricular hypertrophy (LVH) and the transition from compensated LVH to heart failure in a rat model of LVF induced by abdominal aortic coarctation. Furthermore, phosphorylated FAK levels also increased during established phase of compensatory LVH and transition from compensated LVH to heart failure. FAK undergoes tyrosine phosphorylation in response to growth factor stimulation in both cardiomyocytes and smooth muscle cells, and FAK phosphorylation is necessary for activation of downstream signaling cascades leading to cytoskeletal reorganization and cellular growth. Increased FAK expression occurred in both cardiomyocytes and cardiac fibroblast [4].

Earlier we have shown selective induction of either RVH or RVF after 4 weeks of treatment with a low dose (30 mg/kg body weight) or a high dose (80 mg/kg body weight) of MCT, respectively [14]. Here we show that phosphorylation of FAK is significantly increased in MCT-induced RV hypertrophy (RVH) and failure groups (RVF) compared with the control RVC ($p<0.05$ vs. RVC), while the ratio of phosphorylated FAK to total FAK is significantly increased in RVH only ($p<0.05$ vs. RVC).

NO synthase (NOS) is expressed constitutively as two isoforms: endothelial (eNOS) and neuronal (nNOS, NOS1) [30]. Earlier we showed that neuronal nitric oxide synthase (NOS1) is activated by integrin stimulation [32, 33]. NOS1 is located on the SR of cardiomyocytes, and is considered to modify SR function via nitrosylation of the ryanodine receptor which is the calcium release site of the SR [3, 19, 29, 34, 38].

The protein level and the activity of NOS1 have been shown to be enhanced in the LV myocardium of chronically infarcted animals and in failing human hearts [5, 9, 11], suggesting that NOS1 may play a part in the myocardial response to

stress. Furthermore, under these conditions, NOS1 seems to be preferentially localized to the sarcolemmal membrane (rather than to the SR), where it colocalizes with caveolin-3. Bendall *et al*. [5] have shed some light on the functional significance of these findings by showing that under basal conditions NOS1 inhibition increased basal LV inotropy and prolonged the time constant of isovolumic relaxation in sham operated rat hearts, whereas in failing hearts these effects were significantly reduced. In contrast, inhibition of NOS1 enhanced the inotropic and lusitropic response to β-adrenergic stimulation in failing hearts but had no significant effect in sham-operated rats.

In the present study we show that phosphorylated NOS1 as well as the ratio of phosphorylated NOS1 to total NOS1 are significantly increased in MCT-induced RV hypertrophy (RVH) and failure groups (RVF) compared with the control RVC (p<0.05 vs. RVC).

Nitric oxide (NO) and reactive oxygen species produce peroxynitrite, known to activate matrix metalloproteinases (MMPs) [20, 35] that are involved in ventricular remodeling [27]. The stimulating effect of NO on expression of MMP2 and MMP9 has been confirmed in neonatal rat ventricular cardiomyocytes, suggesting that NOS1 activation may be responsible for increased immunoreactivity of MMP-2 and MMP-9. MMPs comprise a family of endopeptidases encompassing more than 25 members able to degrade numerous extracellular matrix components and several intracellular proteins. MMPs are involved in many pathological conditions, including inflammation and different stages of heart failure [6, 28]. In the present study we analysed whether pulmonary hypertension-induced RV failure in rats is associated with an activation of MMP-2 and MMP-9 in RV myocardium.

The structural basis for the development of congestive heart failure (CHF) is a maladaptive myocardial remodeling process which occurs secondarily to post-myocardial infarction (MI), hypertension-induced LV hypertrophy, or cardiomyopathy. Both cellular and extracellular factors are involved in the remodeling process and it is the combined action of these factors giving rise to changes in myocardial structure which eventually affects function. One component in this remodeling process is the MMPs. Many bioactive molecules such as cytokines/chemokines, bioactive peptides, and neurohormones which are operative in CHF likely contribute to the induction of MMPs. For example, a specific cassette of transcription factors is likely induced with extracellular stimuli in the context of CHF which in turn induces MMPs and contributes to the maladaptive remodeling process [12].

MMP-2 and MMP-9 have been shown to be increased in the plasma of patients with heart failure [1]. A study conducted by Banfi *et al.* [2] also demonstrated that plasma levels of both MMP-2 and MMP-9 were elevated in patients with idiopathic and ischemic dilated cardiomyopathy. In another recently conducted study, elevated plasma MMP-9 levels correlated with lower LVEF and higher LVESV [39]. These findings suggest that monitoring of plasma markers of myocardial remodeling may provide important prognostic information with respect to ongoing adverse LV remodeling in patients with heart failure. A study by Tyagi *et al.* [31] also showed an induction of MMP-2 and MMP-9 in ventricular tissues from human heart end-stage failure secondary to ischemic cardiomyopathy. Focusing on the RV myocardium, we found an activation of immunoreactive MMP-2 and MMP-9 in the remodeled RV myocardium of rats with pulmonary hypertension induced RV

failure, suggesting that these MMPs are implicated in RV remodeling. The lower value of MMP-2 immunoreactivity in RV myocardium of rats with RV failure compared to RV myocardium of rats with RV hypertrophy may be due to the release of MMP-2 from the tissue into the circulation, as was reported for MMP-2 concentration in serum of patients with CHF [1,2].
A recent study by Morita *et al.* [21] has shown that selective MMP inhibition attenuates progression of LV dysfunction and remodeling in dogs with CHF.
In conclusion, tyrosine phosphorylation of FAK was most pronounced in hypertrophic RV myocardium whereas phosphorylation of NOS1 was most pronounced in failing RV myocardium, which may point to a role of excessive NO formation in development of failure and an activation of MMPs leading to ventricular remodeling. The exact role of the NO formed in the failing myocardium is not yet fully elucidated.

Acknowledgements

We would like to thank Prof. D.L. Ypey (Dept. of Cardiology, LUMC) for his valuable suggestions regarding the preparation of this manuscript.

References

1. P. Altieri, C. Brunelli, S. Garibaldi, A. Nicolino, S. Ubaldi, P. Spallarossa, L. Olivotti, P. Rossettin, A. Barsotti, G. Ghigliotti. Metalloproteinases 2 and 9 are increased in plasma of patients with heart failure. Eur. J. Clin. Invest. 33 (2003) 648-656.
2. C. Banfi, V. Cavalca, F. Veglia, M. Brioschi, S. Barcella, L. Mussoni, L. Boccotti, E. Tremoli, P. Biglioli, P. Agostoni. Neurohormonal activation is associated with increased levels of plasma matrix metalloproteinase-2 in human heart failure. Eur. Heart J. 26 (2005) 481-488.
3. L.A. Barouch, R.W. Harrison, M.W. Skaf, G.O. Rosas, T.P. Cappola, Z.A. Kobeissi, I.A. Hobai, C.A. Lemmon, A.L. Burnett, B. O'Rourke, E.R. Rodriguez, P.L. Huang, J.A.C. Lima, D.E. Berkowitz, J.M. Hare. Nitric oxide regulates the heart by spatial confinement of nitric oxide synthase isoforms. Nature 416 (2002) 337-340.
4. A.L. Bayer, M.C. Heidkamp, N. Patel, M.J. Porter, S.J. Engman, A.M. Samarel. PYK2 expression and phosphorylation increases in pressure overload-induced left ventricular hypertrophy. Am. J. Physiol. Heart Circ. Physiol. 283 (2002) H695–H706.
5. J.K. Bendall, T. Damy, P. Ratajczak, X. Loyer, V. Monceau, I. Marty, P. Milliez, E. Robidel, F. Marotte, J.L. Samuel, C. Heymes. Role of myocardial neuronal nitric oxide synthase derived nitric oxide in *β*-adrenergic hyporesponsiveness after myocardial infarction-induced heart failure in rat. Circulation 110 (2004) 2368–2375.
6. H. Birkedal-Hansen. Proteolytic remodeling of extracellular matrix. Curr. Opin. Cell Biol. 7 (1995) 728-735.
7. H.P. Buermans, E.M. Redout, A.E. Schiel, R.J. Musters, M. Zuidwijk, P.P. Eijk, C. van Hardeveld, S. Kasanmoentalib, F.C. Visser, S. Ylstra, W.S. Simonides. Microarray analysis reveals pivotal divergent mRNA expression profiles early in the development of either compensated hypertrophy or heart failure. Physiol. Genomics 21 (2005) 314-323.
8. K.N. Cowan, A. Heilbut, T. Humpl, C. Lam, S. Ito, M. Rabinovitch. Complete reversal of fatal pulmonary hypertension in rats by a serine elastase inhibitor. Nat. Med. 6 (2000) 698-702.
9. T. Damy, P. Ratajczak, E. Robidel, J.K. Bendall, P. Olivero, J. Boczkowski, T. Ebrahimian, F. Marotte, J.L. Samuel, C. Heymes. Up-regulation of cardiac nitric oxide synthase 1-derived nitric oxide after myocardial infarction in senescent rats. FASEB J. 17 (2003) 1934–1936.
10. T. Damy, P. Ratajczak, A.M. Shah, E. Camors, I. Marty, G. Hasenfuss, F. Marotte, J.L. Samuel, C. Heymes. Increased neuronal nitric oxide synthase-derived NO production in the failing human heart. Lancet 363 (2004) 1365-1367.
11. D. Dawson, C.A. Lygate, M.H. Zhang, K. Hulbert, S. Neubauer, B. Casadei. nNOS gene deletion exacerbates pathological left ventricular remodeling and functional deterioration after myocardial infarction. Circulation 112 (2005) 3729-3737.
12. A.M. Deschamps, F.G. Spinale. Pathways of matrix metalloproteinase induction in heart failure: Bioactive molecules and transcriptional regulation. Cardiovasc. Res. 59 (2006) 666-676.
13. F. Ghodsi, J.A. Will. Changes in pulmonary structure and function induced by monocrotaline intoxication. Am. J. Physiol. 240 (1981) H149-H155.
14. M.H.M. Hessel, P. Steendijk, B. den Adel, C.I. Schutte, A. van der Laarse. Characterization of right ventricular function after monocrotaline-induced pulmonary hypertension in the intact rat. Am. J. Physiol. Heart Circ. Physiol. 291 (2006) H2424-H2430.
15. A. Hislop, L. Reid. Arterial changes in Crotalaria spectabilis-induced pulmonary hypertension in rats. Br. J. Exp. Pathol. 55 (1974) 153-163.

16. K.M. Ito, M. Sato, K. Ushijima, M. Nakai, K. Ito. Alterations of endothelium and smooth muscle function in monocrotaline-induced pulmonary hypertensive arteries. Am. J. Physiol. Heart Circ. Physiol. 279 (2000) H1786-H1795.
17. M. Laser, C.D. Willey, W. Jiang, G. Cooper IV, D.R. Menick, M.R. Zile, D. Kuppuswamy. Integrin activation and focal complex formation in cardiac hypertrophy. J. Biol. .Chem. 275 (2000) 275: 35624-35630.
18. D.A. MacKenna, F. Dolfi, K. Vuori, E. Ruoslahti. Extracellular signal regulated kinase and c-Jun NH2-terminal kinase activation by mechanical stretch is integrin-dependent and matrix-specific in rat cardiac fibroblasts. J. Clin. Invest. 101 (1998) 301-310.
19. A. Martinez-Ruiz, S. Lamas. S-nitrosylation: a potential new paradigm in signal transduction. Cardiovasc. Res. 62 (2004) 43-52.
20. K. Migita, Y. Maeda, S. Abiru, A. Komori, T. Yokoyama, Y. Takii, M. Nakamura, H. Yatsuhashi, K. Eguchi, H. Ishibashi. Peroxynitrite-mediated matrix metalloproteinase-2 activation in human hepatic stellate cells. FEBS Lett. 579 (2005) 3119-3125.
21. H. Morita, S. Khanal, S. Rastogi, G. Suzuki, M. Imai, A. Todor, V.G. Sharov, S. Goldstein, T.P. O'Neill, H.N. Sabbah. Selective matrix metalloproteinase inhibition attenuates progression of left ventricular dysfunction and remodeling in dogs with chronic heart failure. Am. J. Physiol. Heart Circ. Physiol. 290 (2006) H2522-H2527.
22. H.C. Rosenberg, M. Rabinovitch. Endothelial injury and vascular reactivity in monocrotaline pulmonary hypertension. Am. J. Physiol. 255 (1988) H1484-H1491.
23. R.S. Ross RS, T.K. Borg. Integrins and the myocardium. Circ. Res. 88 (2001) 1112-119.
24. C. Ruwhof, A.E.T. van Wamel, J.M. Egas, A. van der Laarse. Cyclic stretch induces the release of growth promoting factors from cultured neonatal cardiomyocytes and cardiac fibroblasts. Mol. Cell. Biochem. 208 (2000) 89-98.
25. J.Y.J. Shyy, S. Chien. Role of integrins in cellular responses to mechanical stress and adhesion. Curr. Opin. Cell Biol. 9 (1997) 707-713.
26. M.D. Sjaastad, R.S. Lewis, W.J. Nelson. Mechanisms of integrin-mediated calcium signaling in MDCK cells: regulation of adhesion by IP_3- and stress-independent calcium influx. Mol. Biol. Cell. 7 (1996) 1025-1041.
27. F.G. Spinale, M.L. Coker, C.V. Thomas, J.D. Walker, R. Mukherjee, L. Hebbar. Time-dependent changes in matrix metalloproteinase activity and expression during the progression of congestive heart failure. Circ. Res. 82 (1998) 482-495.
28. F.G. Spinale. Matrix metalloproteinases: regulation and dysregulation in the failing heart. Circ. Res. 90 (2002) 520-530.
29. D. Stoyanovski, T. Murphy, P.R. Anno, Y.M. Kim, G. Salama. Nitric oxide activates skeletal and cardiac ryanodine receptors. Cell Calcium 21 (1997) 19-29.
30. M.S. Sumeray, D.D. Rees, D.M. Yellon. Infarct size and nitric oxide synthase in murine myocardium. J. Mol. Cell. Cardiol. 32 (2000) 35-42.
31. S.C. Tyagi, S.G. Kumar, S.J. Haas, H.K. Reddy, D.J. Voelker, M.R. Hayden, T.L. Demmy, R.A. Schmaltz, J.J. Curtis. Post-transcriptional regulation of extracellular matrix metalloproteinase in human heart end-stage failure secondary to ischemic cardiomyopathy. J. Mol. Cell. Cardiol. 28(1996) 1415-1428.
32. A. van der Laarse, C.C. van der Wees, E.J. van der Valk, W.H. Bax. Integrin stimulation induced signaling includes phosphorylation of focal adhesion kinase and nitric oxide synthase-1 leading to elevation of intracellular NO and calcium concentrations in cardiomyocytes. Circulation 112 (Abstract 2005) II-1114.
33. C.G.C. van der Wees, W.H. Bax, E.J.M. van der Valk, A. van der Laarse. Integrin stimulation induces calcium signalling in rat cardiomyocytes by a NO-dependent mechanism. Pflügers Arch. – Eur. J. Physiol. 451 (2006) 588-595.
34. M.G. Vila Petroff, S.H. Kim, S. Pepe, C. Dessy, E. Marban, J.L Balligand, S.J. Sollott. Endogenous nitric oxide mechanisms mediate the stretch dependence of Ca^{2+} release in cardiomyocytes. Nat. Cell Biol. 3 (2001) 867-873.

35. W. Wang, G. Sawicki, R. Schulz. Peroxynitrite-induced myocardial injury is mediated through matrix metalloproteinase-2. Cardiovasc. Res. 53 (2002) 165-174.
36. P.M. Werchan, W.R Summer, A.M. Gerdes, K.H. McDonough. Right ventrcular performance after monocrotaline-induced pulmonary hypertension. Am. J. Physiol. 256(1989) H1328-H1336.
37. D.W. Wilson, H.J. Segall, L.C. Pan, M.W. Lame, J.E. Estep, D. Morin. Mechanisms and pathology of monocrotaline pulmonary toxicity. Crit. Rev. Toxicol. 22 (1992) 307-325.
38. L. Xu, J.P. Eu, G. Meissner, J.S. Stamler. Activation of the cardiac calcium release channel (ryanodine receptor) by poly-S-nitrosylation. Science 279 (1998) 234-237.
39. A.T. Yan, R.T. Yan, F.G. Spinale, R. Afzal, H.R. Gunasinghe, M. Arnold , C. Demers, R.S. Mckelvie, P.P. Liu. Plasma matrix metalloproteinase-9 level is correlated with left ventricular volumes and ejection fraction in patients with heart failure. J. Card. Fail. 12 (2006) 514-519.